THE JOURNAL OF BIOLOGICAL CHEMISTRY VOL. 283, NO. 37, pp. 25381–25391, September 12, 2008

Soybean Nodule Autoregulation Receptor Kinase Phosphorylates Two Kinase-associated Protein Phosphatases *in Vitro*[*] [S]

Received for publication, January 16, 2008, and in revised form, June 30, 2008 Published, JBC Papers in Press, July 7, 2008, DOI 10.1074/jbc.M800400200

Akira Miyahara[‡], Tripty A. Hirani[‡], Marie Oakes[§], Attila Kereszt[‡], Bostjan Kobe[¶1], Michael A. Djordjevic[§], and Peter M. Gresshoff[‡2]

From the [‡]Australian Research Council Centre of Excellence for Integrative Legume Research and [¶]School of Microbial and Molecular Sciences and Institute for Molecular Bioscience, University of Queensland, St. Lucia, Brisbane, Queensland 4072, Australia and the [§]Australian Research Council Centre of Excellence for Integrative Legume Research, Research School of Biological Sciences, Australian National University, Canberra, Australian Capital Territory 2601, Australia

The *NARK* (nodule autoregulation receptor kinase) gene, a negative regulator of cell proliferation in nodule primordia in several legumes, encodes a receptor kinase that consists of an extracellular leucine-rich repeat and an intracellular serine/threonine protein kinase domain. The putative catalytic domain of NARK was expressed and purified as a maltose-binding or a glutathione *S*-transferase fusion protein in *Escherichia coli*. The recombinant NARK proteins showed autophosphorylation activity *in vitro*. Several regions of the NARK kinase domain were shown by mass spectrometry to possess phosphoresidues. The kinase-inactive protein K724E failed to autophosphorylate, as did three other proteins corresponding to phenotypically detected mutants defective in whole plant autoregulation of nodulation. A wild-type NARK fusion protein transphosphorylated a kinase-inactive mutant NARK fusion protein, suggesting that it is capable of intermolecular autophosphorylation *in vitro*. In addition, Ser-861 and Thr-963 in the NARK kinase catalytic domain were identified as phosphorylation sites through site-directed mutagenesis. The genes coding for the kinase-associated protein phosphatases KAPP1 and KAPP2, two putative interacting components of NARK, were isolated. NARK kinase domain phosphorylated recombinant KAPP proteins *in vitro*. Autophosphorylated NARK kinase domain was, in turn, dephosphorylated by both KAPP1 and KAPP2. Our results suggest a model for signal transduction involving NARK in the control of nodule development.

Plant receptor protein kinases (RKs)[3] have been isolated from a number of species, including *Arabidopsis* and rice, and have been suggested to play important roles in signal transduction pathways, such as self-incompatibility, hormone signaling, disease resistance, meristem development, and root nodulation. Most plant RKs are serine/threonine kinases and can be classified into several groups based on their extracellular domain. The leucine-rich repeat (LRR)-RKs comprise the largest family (1). One of the most thoroughly characterized plant LRR-RKs is *Arabidopsis* CLAVATA1 (CLV1) (2). This protein, with 21 LRRs in its extracellular domain, acts to control cell proliferation and cell differentiation in shoot apical meristem. Interacting partners of CLV1, such as the receptor-like protein CLV2 and the ligand peptide CLV3, have been isolated; many aspects of this signaling pathway are thus relatively well understood (3, 4).

The Leguminoseae is the third largest family of flowering plants and includes agronomically and economically important crops, such as soybeans (*Glycine max* (L.) *Merr)*, peas (*Pisum sativum*), and beans (*Phaseolus vulgaris*). Most legumes can engage in symbiosis with nitrogen-fixing soil bacteria, collectively called rhizobia, leading to a sustainable input of nitrogen into the cropping system for food, feed, and fuel production through formation of root nodules. Interestingly, once early cell division for nodule development is induced, autoregulation of nodulation (AON) controls a homeostatic scheme to regulate the nodule number at a level that balances the burden on the plant with the benefits of symbiosis (5). To investigate nodule initiation and AON, research in several legume species has led to the isolation of genes involved in nodulation, such as those encoding Nod factor receptor kinase 1 and 5 (*NFR1* and *NFR5*), symbiosis receptor kinase (*SYMRK*), ion channels *CASTOR* and *POLLUX* from the model legume *Lotus japonicus*, nodule autoregulation receptor kinase (*NARK*) from soybean, and the calcium/calmodulin-dependent protein kinase (*DMI3*) from *Medicago truncatula* (6–11).

[*] This work was supported by the Australian Research Council Centre for Integrative Legume Research, the Queensland State Government Smart State Innovation Scheme, and the University of Queensland. The costs of publication of this article were defrayed in part by the payment of page charges. This article must therefore be hereby marked "*advertisement*" in accordance with 18 U.S.C. Section 1734 solely to indicate this fact.

[S] The on-line version of this article (available at http://www.jbc.org) contains supplemental Fig. 1.

The nucleotide sequence(s) reported in this paper has been submitted to the GenBank™/EBI Data Bank with accession number(s) EU350557, EU350554, EU350558, and EU350555.

[1] An Australian Research Council Federation Fellow and a National Health and Medical Research Council Honorary Research Fellow.

[2] To whom correspondence should be addressed: CILR, The University of Queensland, St. Lucia, Brisbane, Queensland 4072, Australia. Tel.: 61-7-3365-3550; Fax: 61-7-3365-3556; E-mail: p.gresshoff@uq.edu.au.

[3] The abbreviations used are: RK, receptor kinase; KI, kinase-interacting; FHA, forkhead-associated; PP2C, protein phosphatase 2C; AON, autoregulation of nodulation; BAC, bacterial artificial chromosome; RACE, rapid amplification of cDNA ends; MBP, maltose-binding protein; GST, glutathione *S*-transferase; MyBP, myelin basic protein; LRR, leucine-rich repeat; aa, amino acid(s); MALDI, matrix-assisted laser desorption ionization; TOF, time-of-flight; KD, kinase domain.

Induction of nodule primordia appears to trigger the AON cascade (5). If AON is interrupted, supernodulation or hypernodulation occurs. The *NARK* gene in soybean (and homologues in other legumes) plays a central role in AON. It encodes an LRR-RK composed of a signal peptide, 19 tandem LRRs, a transmembrane region, and a cytoplasmic kinase domain (8). So far, orthologues of *NARK* have been isolated from *L. japonicus* (*HAR1*), *M. truncatula* (*SUNN*), and *P. sativum* (*SYM29*) (12–14). However, no biochemical evidence of the kinase activity of any AON LRR-RKs has yet been reported, although autophosphorylation and transphosphorylation ability would be predicted to play a critical role in AON. To date, autophosphorylation of some plant RKs (expressed in and purified from *Escherichia coli*) has been confirmed, and the phosphorylation sites of some of those RKs, such as BRI1, SERK1, XA21, and SYMRK, have been identified (15–18).

KAPP (kinase-associated protein phosphatase), originally isolated from *Arabidopsis*, is a negative regulator of signal transduction and interacts with phosphorylated kinase domains of several RKs, including CLV1, HAESA, RLK4, FLS2, BRI1, BAK1, and SERK1 (19–25). Although *KAPP* orthologues have been isolated from maize and rice (22, 26), no homologue of *KAPP* had been identified in legume genomes up to now. The KAPP protein is composed of three major domains: an N-terminal type 1 signal anchor, a kinase-interacting (KI) domain containing a forkhead-associated (FHA) domain, and a type 2C protein phosphatase (PP2C) domain. The N-terminal signal anchor localizes *Arabidopsis* KAPP to the cytoplasmic surface of the plasma membrane. The KI domain has been demonstrated to bind *in vitro* to catalytic domains of several RKs in a phosphorylation-dependent manner (21, 22, 24). The minimal KI domain of *Arabidopsis* KAPP was defined as a 119-amino acid (aa) segment (27). It has been hypothesized that the KAPP KI domain brings the KAPP PP2C domain close to its phosphorylated RK target to attenuate RK signaling by dephosphorylation (28).

Here, we investigated the biochemical properties of NARK. Residues in the NARK protein important for its kinase activity were defined by coupling site-directed mutagenesis and *in vitro* phosphorylation assays. In addition, NARK regions containing phosphate modifications were determined by mass spectrometry. Furthermore, we isolated two soybean *KAPP* genes, *KAPP1* and *KAPP2*, and demonstrated that KAPP1 and KAPP2 are phosphorylated by NARK and that in turn they are capable of dephosphorylating NARK *in vitro*.

EXPERIMENTAL PROCEDURES

NARK-KD Constructs—The kinase catalytic domain (aa 663–987) of NARK (GenBank™ accession number AY166655) was amplified from leaf cDNA by PCR using the forward primer 5′-GGCGGTGACGGAATTCTAGTGTACATGATGAGGAGGAGGAA-3′ and the reverse primer 5′-GCTTAACTATGTCGACCTAGAGATTAATTAGGTTGTGAGTGTGA-3′. The product was ligated into the EcoRI/SalI sites of the glutathione *S*-transferase (GST) fusion vector, pGEX-KG (29), resulting in GST-NARK-KD, which is composed of the juxtamembrane domain, the kinase domain, and the C-terminal region. Also, the same region of the NARK kinase catalytic domain (as for the GST fusion) was amplified by PCR using the forward primer 5′-GGCGGTGACGGAATTCGTGTACATGATGAGGAGGAGGAA-3′ and the same reverse primer as described above. The PCR product was digested with EcoRI and SalI and cloned into the maltose-binding protein (MBP) fusion vector, pMALc2x (New England Biolabs), resulting in MBP-NARK-KD, which is composed of the juxtamembrane domain, the kinase domain, and the C-terminal region.

GST-NARK-KD and MBP-NARK-KD Mutant Constructs—Mutations were introduced in GST-NARK-KD or MBP-NARK-KD using PCR-based site-directed mutagenesis (30). PCR products containing the mutations K724E, S731A, S861A, T872A, S936A, and T963A were cloned into pGEX-KG using EcoRI/SalI sites, resulting in the GST-NARK-K724E, GST-NARK-S731A, GST-NARK-S861A, GST-NARK-T872A, GST-NARK-S936A, and GST-NARK-T963A constructs. PCR products containing the mutations K724E, E741K, V837A, and R961K were cloned into pMALc2x vector using EcoRI/SalI sites, resulting in MBP-NARK-K724E, MBP-NARK-E741K, MBP-NARK-V837A, and MBP-NARK-R961K.

Isolation of KAPP1 and KAPP2 from Soybean—Partial sequences encoding KAPP1 and KAPP2 were identified from a soybean expressed sequence tag data base by the tBLASTn program (31) using the *Arabidopsis* KAPP protein sequence (U09505) as a template. The *KAPP1* and *KAPP2* genes were partially amplified from soybean genomic DNA by PCR and labeled with [α-^{32}P]dATP. Bacterial artificial chromosome (BAC) clones 0111O22 and 0015J20, containing the *KAPP1* and *KAPP2* genes, respectively, were isolated from a BAC library (GM_PBa) derived from soybean line PI437654 (Clemson University Genomics Institute) by filter hybridization to ^{32}P-labeled probes. Total RNA was isolated from soybean leaves, and whole cDNA sequences of *KAPP1* and *KAPP2* were determined by 5′- and 3′-rapid amplification of cDNA ends (RACE) (Invitrogen). cDNA sequences of *KAPP1* and *KAPP2* were amplified by PCR and cloned into the pCR2.1-TOPO vector (Invitrogen). Genomic sequences were determined from BAC clones listed above. Both genomic and cDNA sequences of *KAPP1* and *KAPP2* were deposited in GenBank™: *KAPP1* genomic sequence, EU350557; *KAPP1* cDNA sequence, EU350554; *KAPP2* genomic sequence, EU350558; *KAPP2* cDNA sequence, EU350555.

KAPP1 and KAPP2 Constructs—cDNAs encoding aa 46–576 for KAPP1 and aa 46–578 for KAPP2 (corresponding to the proteins lacking the N-terminal signal anchor) were amplified by PCR using the forward primer 5′-CTCCATCAAGGGCTCTAGACGAGCTAGAGCGGCCCCTTTT-3′ and the reverse primer 5′-CTAATTCATAGTCGACCTAGGATTCAACTTTACAAGAGAATCTG-3′. The PCR products of *KAPP1* and *KAPP2* were digested with XbaI and SalI and cloned into the pGEX-KG vector, resulting in GST-KAPP1 and GST-KAPP2, respectively.

Expression and Purification of Recombinant Fusion Proteins—Each construct for protein expression was transformed into *E. coli* strain Rosetta (Novagen®; EMD Biosciences). A 10-ml overnight culture was transferred to 500 ml of LB for GST constructs and to rich medium (1% tryptone, 0.5% yeast extract, and 0.5% NaCl) containing 0.2% glucose for MBP constructs.

The cells were cultured at 37 °C to a density of about 0.8 A_{600}. Expression of GST and MBP recombinant fusion proteins was induced with 0.1 mM and 1.0 mM isopropyl-D-thiogalactopyranoside, respectively, for 16 h at 20 °C. The cells were collected by centrifugation and resuspended in the lysis buffer (50 mM HEPES (pH 7.4), 150 mM NaCl, 1 mM phenylmethylsulfonyl fluoride, 1 mM benzamidine for GST fusion proteins and 10 mM Na_2PO_4 (pH 7.2), 500 mM NaCl, 0.25% Tween 20, 10 mM β-mercaptoethanol, 1 mM phenylmethylsulfonyl fluoride, 1 mM benzamidine for MBP fusion proteins). All GST and MBP fusion proteins were purified by affinity chromatography on either glutathione-Sepharose 4B (GE Healthcare) for GST or amylose resin (New England Biolabs) for MBP as described by Horn and Walker (32) with the following modifications. The cleared extract was incubated for 2–4 h at 4 °C, and the beads were collected and washed by the lysis buffer on a column. The GST or MBP recombinant fusion proteins were eluted by adding either GST elution buffer (50 mM HEPES and 15 mM glutathione (pH 8.0) or MBP elution buffer (10 mM Na_2PO_4 (pH 7.2), 500 mM NaCl, 0.25% Tween 20, 10 mM β-mercaptoethanol, 10 mM maltose), respectively. GST-NARK-S861A was eluted in the GST elution buffer with the addition of 150 mM NaCl. The purified recombinant fusion proteins, excluding GST-NARK-KD and the GST-NARK-KD mutants, were dialyzed against 20 mM TES (pH 7.2) and then stored in 10% glycerol at −20 °C. The GST-NARK-KD and GST-NARK-KD mutant proteins were stored directly in 10% glycerol at −20 °C.

Autophosphorylation and Transphosphorylation Assays—Autophosphorylation assays were performed by incubating either 500 ng of GST-NARK-KD proteins or 1 μg of MBP-NARK-KD proteins in 50 mM HEPES (pH 7.4), 50 mM NaCl, 1 mM dithiothreitol, 10 mM $MnCl_2$, 50 μM unlabeled ATP, and 10 μCi of [γ-^{32}P]ATP in a 20-μl reaction at 25 °C for 1 h. The reaction was terminated by adding SDS-PAGE sample buffer and boiling at 95 °C for 5 min, and then protein samples were separated by 10 or 12% SDS-PAGE. The gels were stained by Coomassie Brilliant Blue R250, destained, and dried using a gel dryer. The radioactivity was quantified by a PhosphorImager (STORM™; GE Healthcare), and data were analyzed using the ImageQuant program (GE Healthcare). Transphosphorylation assays were carried out under the same condition as described above with the reaction buffer containing 10 mM $MgCl_2$ and either 1 μg of a GST fusion protein or 1 μg of nonnatural substrates (*e.g.* casein, histone, or myelin basic protein (MyBP)). The transphosphorylation assays between GST-NARK-KD and MBP-NARK-KD mutants were performed by incubation at 25 °C for 90 min. GST-NARK-S861A was eluted in a buffer containing 150 mM NaCl, whereas no salt was used for other proteins. To confirm whether the difference of the salt concentration in the elution buffer affected the results of phosphorylation assays, we repeated the phosphorylation assay in the presence of salt and found it had no effect (data not shown). Here and throughout, all experiments were repeated independently at least twice.

Dephosphorylation Assay—Cells containing the GST-NARK-KD construct were induced, and the expressed protein was purified on glutathione-Sepharose 4B resin as described above. Before eluting the protein, the resin-bound kinase was autophosphorylated with [γ-^{32}P]ATP for 90 min at 25 °C. Unbound label was removed by washing four times with 50 mM HEPES (pH 7.4). The phosphorylated GST-NARK-KD was eluted with a buffer containing 50 mM HEPES and 15 mM glutathione (pH 8.0) and stabilized with 10% glycerol. Aliquots of the phosphorylated GST-NARK-KD were incubated with 1.5 μg of GST-KAPP1, GST-KAPP2, or GST in 50 mM Tris (pH 7.0), 0.1% β-mercaptoethanol, and 10 mM divalent cation at 25 °C for 4 h. For the time course assay, aliquots were taken at time intervals of 0, 120, and 240 min. The radioactivity was quantified as described above.

Tertiary Structure Predictions—The tertiary structure of the NARK kinase domain (aa 666–987) was predicted using the TASSER-Lite package (available on the World Wide Web) (33, 34) consisting of TASSER, PROSPECTOR_3, SPICKER, and PULCHRA programs and as a template a Protein Data Bank file with the best score (type I transforming growth factor β serine/threonine receptor (Protein Data Bank code 1b6c) (35) with Z-score of 19.289). The structure was visualized using the Swiss-Pdb Viewer program (36).

Mass Spectrometry and Phosphopeptide Purification—The identity and properties of wild-type GST and MBP-NARK-KD fusion proteins were determined prior to and after the addition of ATP using an ABI 4800 MALDI-TOF/TOF mass spectrometer (Applied Biosystems) (37). Individual protein bands of the fusion proteins were excised from one-dimensional SDS-polyacrylamide gels stained with Coomassie Brilliant Blue G250, trypsin-digested, and, if necessary, subjected to C18 Zip tip clean up before analysis (38, 39). Phosphopeptides were enriched from trypsin-digested samples of fusion proteins with and without exposure to ATP using PhosTrap beads following the manufacturer's protocols (PerkinElmer Life Sciences). Putative phosphopeptides enriched by the PhosTrap beads were identified by mass spectrometry and confirmed by neutral loss of multiples of 98 Da. Proteins were identified using Mascot software (Matrix Science, London, UK) at the Australian Proteomic Computational Facility (available on the World Wide Web), by searching against the soybean expressed sequence tag data base (Soy gene index 12.0; September 2004) and the nonredundant data base (MSDB). The mass tolerance was set at 0.3 Da with variable modifications allowed for cysteine (carbamidomethyl) and methionine (oxidation) and one or two trypsin miscleavages. Protein matching and phosphopeptide analysis were done from at least three independent samples.

RESULTS

Characterization of NARK Kinase Activity—We expressed the kinase catalytic domain of NARK as GST and MBP fusion proteins in *E. coli*. We first determined the dependence on divalent cations of GST-NARK-KD for autophosphorylation activity. In this assay, either the chloride salt of Mg^{2+}, Mn^{2+}, or Ca^{2+} or a combination of two of the ions were used (Fig. 1*A*). The results indicate that the autophosphorylation activity of GST-NARK-KD requires $MnCl_2$ for its maximum activity, followed by $MgCl_2$. Autophosphorylation activity was not observed when the GST-NARK-KD protein was incubated with $CaCl_2$ or in the absence of cations (data not shown). The addition of either $MgCl_2$ or $CaCl_2$ to $MnCl_2$ neither promoted

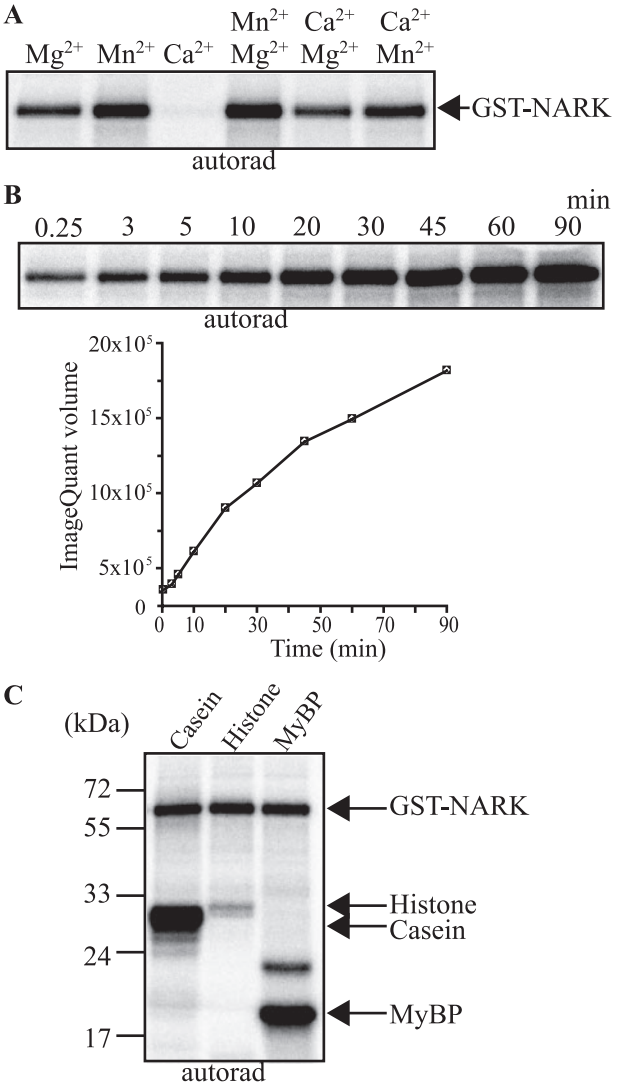

FIGURE 1. **Phosphorylation by GST-NARK-KD.** *A*, the GST-NARK-KD protein was subjected to autophosphorylation in the presence of different divalent cations. GST-NARK-KD was incubated with divalent cations ($MgCl_2$, $MnCl_2$, $CaCl_2$, $MgCl_2$ and $MnCl_2$, $MgCl_2$ and $CaCl_2$, and $MnCl_2$ and $CaCl_2$; 10 mM concentration). *B*, time course of the GST-NARK-KD autophosphorylation activity. The GST-NARK-KD protein was incubated in the presence of $MnCl_2$ at 25 °C from 0.25 to 90 min. The quantified ImageQuant volume of the GST-NARK-KD autophosphorylation is shown *below* the autoradiograph image. *C*, phosphorylation of nonnatural substrates by GST-NARK-KD. 1 μg of casein, histone, and MyBP was incubated with GST-NARK-KD protein and [γ-^{32}P]ATP at 25 °C for 60 min.

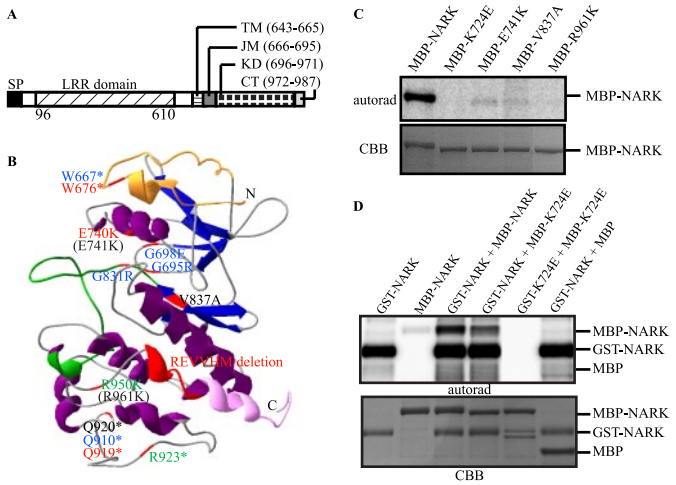

FIGURE 2. **Mutations affect the phosphorylation activity of NARK.** *A*, schematic diagram of NARK protein. *SP*, signal peptide; *LRR*, leucine-rich repeat domain; *TM*, transmembrane domain; *JM*, juxtamembrane domain; *KD*, cytoplasmic serine/threonine kinase domain; *CT*, C-terminal domain. The NARK protein has a molecular mass of 108.9 kDa. *B*, predicted tertiary structure model of the NARK catalytic domain. A model of the NARK catalytic domain (aa 666–987) was constructed by the TASSER-Lite program. The position of the mutations in the AON LRR-RK mutants, *nark*, *har1*, *sym29*, and *sunn*, shown in Table 1 are indicated in *red*. The *nark* mutations are shown in *black* (V837A and Q920*), *har1* in *red* (W676*, E740K, Q919*, and REVVHM deletion), *sym29* in *blue* (W667*, G695R, G698E, G831R, and Q910*), and *sunn* in *green* (R923* and R950K), respectively. *Asterisks* represent stop codons. Two *nark* mutations used in *C* are shown in *black* with *brackets* (E741K and R961K). β-Strands and helices are indicated in *blue* and *purple*, respectively. The juxtamembrane region, activation loop, and C-terminal region are highlighted in *yellow*, *green*, and *pink*, respectively. *C*, 1 μg of MBP-NARK-*KD* and four missense mutant MBP-NARK-KD proteins (E741K, V837A, R961K, and K724E) were incubated with [γ-^{32}P]ATP and 10 mM $MnCl_2$ for 1 h at 25 °C. The proteins were separated by SDS-PAGE and visualized by Coomassie Brilliant Blue R250 (*CBB*). The gels were autoradiographed using the PhosphorImager after drying. *D*, GST-NARK-KD transphosphorylates the MBP-NARK-KD proteins. 500 ng of MBP-NARK-KD and MBP-NARK-K724E "kinase-inactive" mutant were incubated with 500 ng of GST-NARK-KD protein with 10 μCi of [γ-^{32}P]ATP, 10 mM $MgCl_2$, and 10 mM $MnCl_2$ for 90 min at 25 °C.

nor inhibited GST-NARK-KD autophosphorylation activity. Autophosphorylation of GST-NARK-KD was increased in a time-dependent manner in a standard condition containing 10 mM $MnCl_2$ (Fig. 1*B*). The phosphorylation activity of NARK was also tested using nonnatural substrates known to be modified by other kinases. The GST-NARK-KD protein was incubated with either casein, histone, or MyBP in a kinase buffer containing both 10 mM $MgCl_2$ and 10 mM $MnCl_2$. The results showed that both casein and MyBP were strongly phosphorylated by the GST-NARK-KD, whereas histone was a poor substrate (Fig. 1*C*).

The six domains of the predicted NARK protein are shown in Fig. 2*A*. Although all AON LRR-RKs, including NARK, SUNN, and HAR1, are predicted to have the same structural characteristics, no tertiary structures of AON RKs have as yet been reported. To help understand the structure-function relationship of such AON kinases, a model of the NARK kinase catalytic domain was built by the TASSER-Lite program suite (33, 34), which performs a threading template assembly/refinement approach. PROSPECTOR_3 in the suite identified a set of 20 homologous templates for the NARK catalytic domain model with high Z-scores. The highest scoring template was the cytoplasmic domain of the type I transforming growth factor β serine/threonine receptor (Protein Data Bank code 1b6c) (35). The best of five cluster models generated by the TASSER-Lite program was selected, and the positions of the mutations from *nark*, *har1*, *sym29*, and *sunn* mutants (Table 1) were mapped onto this tertiary structure (Fig. 2*B*). Most of the mutations in the kinase catalytic domain of AON RKs are likely to affect the kinase activities. To demonstrate this experimentally, E740K, V837A, and R950K mutants based on existing super- or hypernodulation mutants, *har1-5*, *nts1116*, and *sunn1* (14, 40, 41), were selected, and the corresponding residues were mutated in the MBP-NARK-KD, resulting in MBP-NARK-E741K, -V837A, and -R961K mutants. Another mutant (K724E) was created by changing a conserved lysine in subdomain II to a glutamic acid (Fig. 2*C*). All of the protein mutants had greatly reduced autophosphorylation activity. The relative autophos-

TABLE 1
AON LRR-RK mutant alleles in the kinase catalytic domain
Asterisks represent stop codons.

Gene	Allele	Mutation	Identical position in NARK	Domain	Reference
G. maxnark	*nts382*	Q920*	NA[a]	X	8
	nts1116	V837A	NA	VII	8
L. japonicus har1	*har1-1*	W676*	Trp-677	JM	12
	har1-2	Q919*	Gln-920	X	12
	har1-3	964–969 deletion	965–970	XI	12
	har1-5	E740K	Glu-741	III	13
P. sativum sym29	*p87*	G831R	Gly-841	VII	12
	p89, p94, p117	Q910*	Gln-920	X	12
	p90	G695R	Gly-705	I	12
	p91	G698E	Gly-708	I	12
	p116	W667*	Trp-677	JM	12
M. truncatula sunn	*sunn1*	R950K	Arg-961	XI	14
	sunn3	R923*	Arg-934	X	14

[a] Not applicable.

phorylation activity of the MBP-NARK-K724E, -E741K, -V837A, and -R961K mutant proteins was 1.2, 7.2, 2.5, and 1.5% of the wild-type MBP-NARK-KD protein activity (based on a relative ImageQuant volume obtained after PhosphorImager scanning of the gel containing the radiolabeled proteins). Moreover, the mutant proteins migrated differently from the wild-type protein on SDS-PAGE (Fig. 2*C*); the differences of protein migration were most likely to be caused by the differential phosphorylation status.

To investigate whether NARK phosphorylates itself, MBP-NARK-K724E kinase-deficient protein and MBP-NARK-KD wild-type protein were used as substrates for phosphorylation by GST-NARK-KD (Fig. 2*D*). The results showed that the GST-NARK-KD appeared to transphosphorylate the MBP-NARK-KD mutant protein. This suggests that autophosphorylation of NARK *in vitro* can occur in *trans*. In this assay, MBP-NARK-KD showed a much weaker autophosphorylation activity compared with GST-NARK-KD on the same gel. This might have been caused by the rather large molecular tag, MBP (about 45 kDa) in the MBP-NARK-KD, blocking the NARK-KD protein (about 34 kDa) from autophosphorylating efficiently.

Determination of Potential Phosphorylation Sites of NARK in Vitro via Site-directed Mutagenesis—Using comparative sequence analysis, modeling and phosphorylation site prediction programs (Predikin (available on the World Wide Web) (42) and NetPhos2.0 (available on the World Wide Web) (43)), residues Ser-731, Ser-861, Thr-872, Ser-936 and Thr-963 were identified as potential phosphorylation sites of the NARK kinase catalytic domain. Residue Ser-861 corresponds to Thr-468 in AtSERK1, Thr-760 in LjSYMRK, and Thr-1049 in AtBRI1, and all are located in the activation loop. A serine or threonine residue at this position is highly conserved among most serine/threonine kinases and has been reported to be involved in phosphorylation events in the case of AtSERK1 (16, 24), LjSYMRK (17), and AtBRI1 (44). Thr-872 in the NARK catalytic domain corresponds to Thr-868 in AtCLV1 that lies in the first loop after the activation loop and was previously predicted to be involved in the interaction with the AtKAPP KID-FHA domain (25). All five candidate residues were substituted by Ala using site-directed mutagenesis (Fig. 3*A*). GST-NARK-S731A, S861A, T872A, and T963A mutant proteins were subjected to autophosphorylation along with wild-type GST-NARK-KD and the

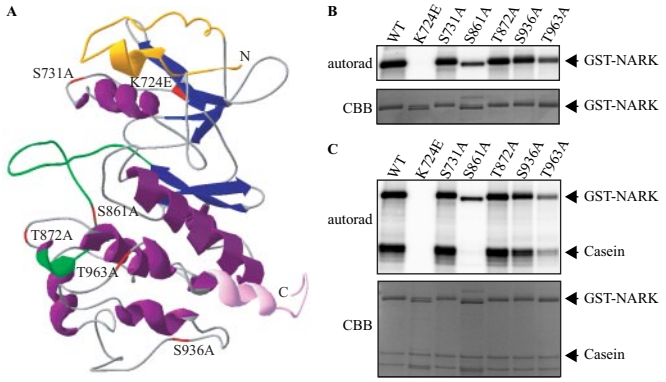

FIGURE 3. **Effects of mutations on the predicted phosphorylation sites of GST-NARK-KD.** *A*, position of mutations in the NARK tertiary structure model. Residues mutated in this study are *highlighted* in *red*. *B*, GST-NARK-KD serine/threonine mutants (S731A, S861A, T872A, S936A, and T963A), a kinase-inactive mutant (K724E), and wild-type GST-NARK-KD protein were subject to autophosphorylation. *C*, the same proteins as used in *B* were incubated with 1 μg of casein in kinase buffer containing 10 mM $MgCl_2$ and 10 mM $MnCl_2$. *CBB*, Coomassie Brilliant Blue.

GST-NARK-K724E kinase-inactive mutant as controls (Fig. 3*B*). Autophosphorylation was reduced considerably in the S861A mutant (29% remaining activity relative to wild type; *i.e.* 71% inhibition) and in the T963A mutant (24% relative to wild type), whereas it was reduced to an intermediate level in the S936A mutant (49% relative to wild type). We observed small reductions in autophosphorylation in two other mutants (71% for S731A and 73% for T872A relative to wild type).

The ability of the various fusion protein derivatives to transphosphorylate casein was determined (Fig. 3*C*). Transphosphorylation of casein was abolished in the S861A mutant (2.8% relative to wild type), whereas it was reduced considerably in the T963A mutant (24% relative to wild type). There was some reduction in the case of the S936A mutant (62% relative to wild type). However, there was no significant reduction in the S731A and in the T872A mutants (94 and 97%, respectively).

Determination of Potential Phosphorylation Sites of NARK in Vitro Using Mass Spectrometry—The results of MALDI-TOF/TOF mass spectrometry for the wild-type GST- and MBP-NARK-KD fusion proteins confirmed the identity of the fusion proteins (Fig. 4*A*). Phosphopeptides were enriched from ATP exposed and nonexposed samples of GST- and MBP-NARK-KD fusion proteins. Seven peptides (some overlapping)

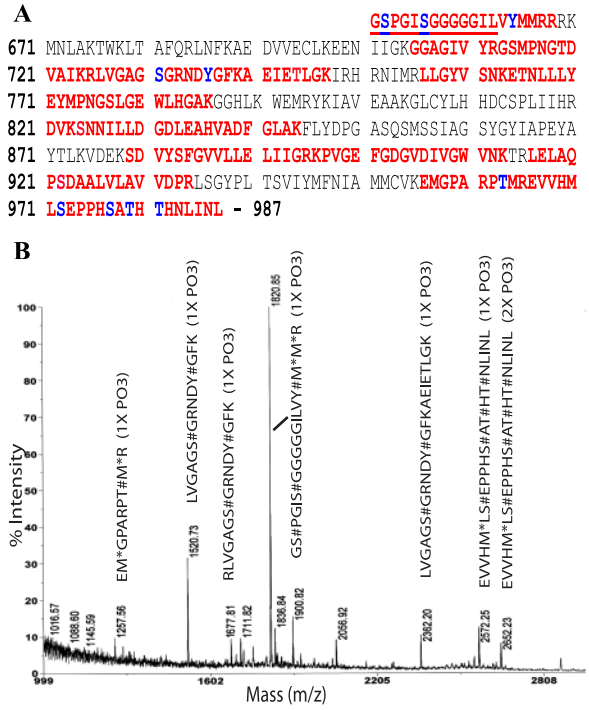

FIGURE 4. **Mass spectrometry analysis of the NARK fusion proteins.** *A*, the tryptic peptides of NARK derived from the analysis of the GST-NARK-KD or MBP-NARK-KD fusion proteins were identified by MALDI-TOF/TOF analysis and are shown in *red*. The *underlined sequence* is derived from the GST linker. Tryptic digestion of the GST-NARK-KD fusion protein generates a peptide that spans the linker sequence to the arginine in the NARK-KD at position 668. Possible phosphorylation sites in the phosphopeptides are indicated in *blue*. *B*, a representative MALDI-TOF/TOF spectrum resulting after purification of phosphopeptides from GST-NARK-KD. The spectra obtained from GST-NARK-KD peptides purified from PhosTrap beads were identical, irrespective of whether the fusion protein was incubated with ATP or not. The sequences of the corresponding phosphopeptides are shown. All of the phosphopeptides indicated showed the neutral loss of 98 daltons (indicating the presence of a single phosphate residue) except for the peak at 2652, which has two phosphoresidues. The inferred or possible sites of phosphorylation are marked in *B* by a *number symbol*, and oxidation of Met is marked by an *asterisk*.

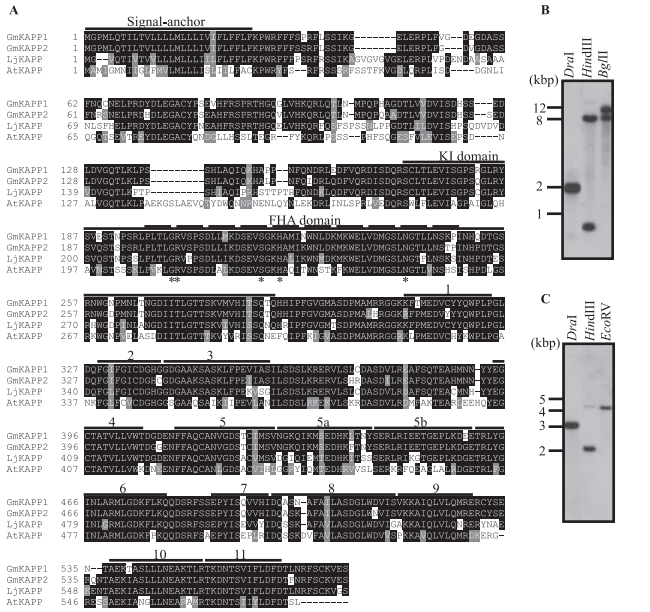

FIGURE 5. *A*, alignment of the KAPP proteins (GmKAPP1, GmKAPP2, LjKAPP, and AtKAPP). Signal anchor, KI domain, and 11 conserved PP2C motifs are indicated by *lines*. The position of FHA domains is shown by a *broken line*, and the invariant residues on FHA domains are represented by *asterisks*. *B*, Southern blot of genomic DNA from soybean probed with the cDNA fragment corresponding to the KAPP1 KI domain. Genomic DNA was digested with DraI, HindIII, and BglII. *C*, Southern blot of genomic DNA from *L. japonicus* probed with the cDNA fragment corresponding to the LjKAPP KI domain. Genomic DNA was digested with DraI, HindIII, and EcoRV.

were shown to carry one or two phosphate modifications (indicated by #) that collectively covered two or possibly three separate regions of the NARK kinase catalytic domain (Fig. 4*B*). The first region incorporated two adjacent C-terminal tryptic fragments between aa 956 and 987 (^{956}EMGPARPT#MR^{965} and the adjacent C-terminal peptide ^{966}EVVHMLS#EPPHS#AT#HT#HNLILN^{987}). Thr-963 is the most likely site for phosphorylation in the aa 956–965 peptide (Fig. 4, *A* and *B*). In contrast, the aa 966–987 peptide contained four possible phosphorylation sites but was found to have either one or two phosphate residues; therefore, the precise site could not be determined (Fig. 4, *A* and *B*). The second region centered on several overlapping tryptic peptides spanning aa 724–739 (^{724}KRLVGAGS#GRNDY#GFK^{739}). This region was found with only one phosphate modification, but two sites are candidates for the locations of these phosphates (Fig. 4, *A* and *B*). A possible third region included a peptide spanning the GST linker and the NARK juxtamembrane domain. This peptide was found only in tryptic digests of GST-NARK-KD (GST linker –GS#PGIS#GGGGILVY#MMR^{667}) (Fig. 4, *A* and *B*). Tyr-664 is the only possible NARK amino acid for phosphorylation in the NARK juxtamembrane domain peptide, but the two Ser residues in the GST linker cannot be ruled out (Fig. 4, *A* and *B*). The inability of trypsin to cut at Arg-733 and Arg-961 is most likely due to steric hindrance of trypsin by the nearby phosphomodifications (at either Ser-731, Tyr-736, or Thr-963; Fig. 4*B*). The phosphopeptides identified in GST-NARK-KD or MBP-NARK-KD with or without ATP present were indistinguishable (data not presented), suggesting that autophosphorylation of GST- and MBP-NARK-KD fusion proteins can occur in *E. coli*. The putative locations of the phosphomodifications need to be confirmed independently using direct strategies.

Isolation of Soybean KAPPs—A possible downstream regulator of several RKs in plants is KAPP, originally isolated as an interacting partner of HAESA (formerly known as RLK5) in *Arabidopsis* and reported to interact with CLV1 as well as several other RKs. Because NARK, previously labeled as soybean CLV1B, shares high similarity with *Arabidopsis* CLV1, we speculated that NARK might interact with the soybean homologue of KAPP. Because no soybean *KAPP* genes had been reported, we screened the soybean BAC library with the partial soybean *KAPP* sequences. In parallel, their full-length cDNA sequences were determined by 5′- and 3′-RACE from cultivar Bragg. The number of genes related to *KAPP* in the soybean genome were surveyed by DNA gel blot analysis using a *KAPP1* cDNA probe that encodes the KI domain (Fig. 5*B*). The results of the Southern hybridization and BAC screening suggested that the soybean genome contains two *KAPP* genes (consistent with its ancestral allotetraploid nature), unlike species such as *Arabidopsis*, maize, and rice, where it exists as a single copy (21, 22, 45).

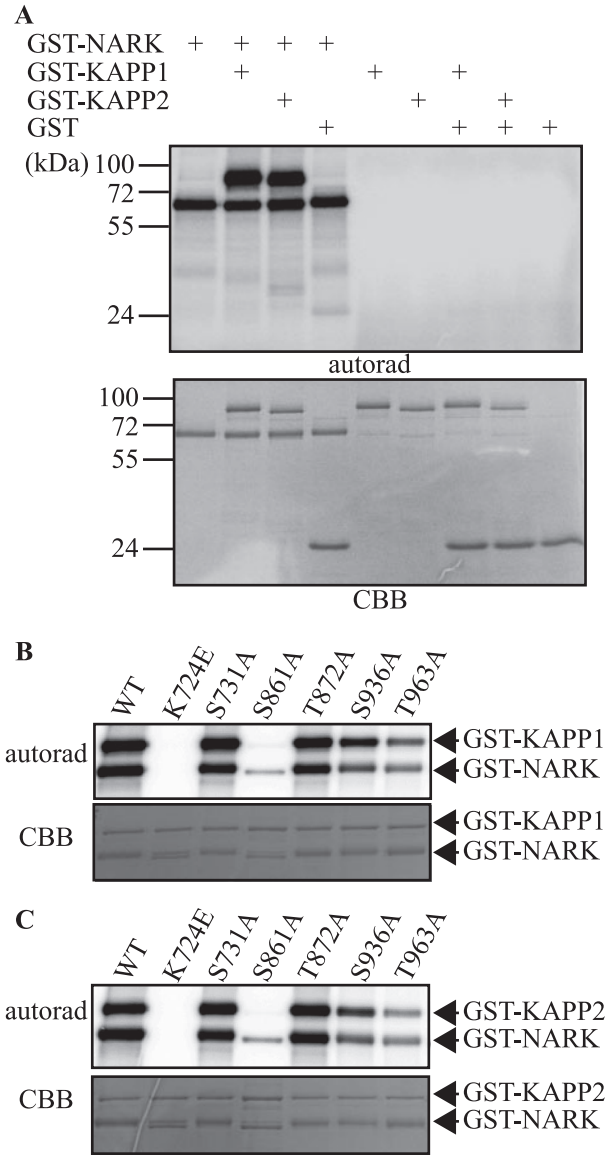

FIGURE 6. **Transphosphorylation between NARK and KAPP proteins.** *A*, the indicated proteins (GST-NARK-KD, GST-KAPP1, GST-KAPP2, and GST) were subjected to *in vitro* phosphorylation assay either alone or in combination. The samples were separated by SDS-PAGE, stained with Coomassie Brilliant Blue (*CBB*), dried, and autoradiographed using the PhosphorImager. *B* and *C*, the GST-NARK-KD and mutants were incubated with GST-KAPP1 (*B*) and GST-KAPP2 (*C*), respectively. After a 60-min incubation at 25 °C, protein samples were separated by SDS-PAGE, and the radioactive bands were detected by the PhosphorImager. *WT*, wild type.

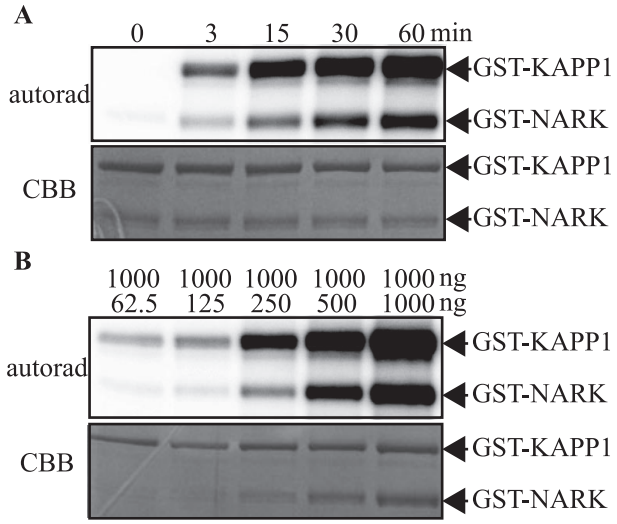

FIGURE 7. **Transphosphorylation of NARK and KAPP1 proteins.** *A*, time course of the GST-NARK-KD transphosphorylation activity. 500 ng of the GST-NARK-KD protein was incubated with 1 μg of GST-KAPP1 at 25 °C from 0 to 60 min. *B*, different concentrations of GST-NARK-KD (from 62.5 ng to 1 μg) were incubated with 1 μg of GST-KAPP1 at 25 °C for 60 min. *CBB*, Coomassie Brilliant Blue.

KAPP1 and KAPP2 comprise 576 and 578 amino acids, respectively. Similar to other KAPP proteins, the soybean KAPP1 and KAPP2 contain an N-terminal signal anchor, a KI domain containing an FHA domain, and a PP2C domain (Fig. 5*A*). The KAPP1 protein is 93% identical to the KAPP2 protein; KAPP1 and KAPP2 proteins are 58 and 57% identical to *Arabidopsis* KAPP, respectively. Specifically, KAPP1 and KAPP2 share 67 and 68% sequence identity, respectively, with *Arabidopsis* KAPP across the KI domain and 65 and 64% sequence identity with *Arabidopsis* KAPP across the PP2C domain.

Phosphorylation of KAPP1 and KAPP2—To investigate whether both KAPP1 and KAPP2 are substrates of the NARK kinase catalytic domain, transphosphorylation assays were carried out. For this purpose, recombinant GST fusion proteins of KAPP1 and KAPP2, lacking the N-terminal signal anchor, were incubated with GST-NARK-KD in the presence of [γ-^{32}P]ATP. The results of the *in vitro* phosphorylation assay showed that GST-NARK-KD phosphorylated both GST-KAPP1 and GST-KAPP2 but not GST alone (Fig. 6*A*). Furthermore, to test whether serine/threonine mutations in GST-NARK-KD affected the phosphorylation of the proteins, we incubated GST-KAPP1 or GST-KAPP2 with GST-NARK-K724E, -S731A, -S861A, -T872A, -S936A, and -T963A mutants (Fig. 6, *B* and *C*). KAPP proteins were phosphorylated by the S731A, T872A, S936A, and the T963A mutant proteins; however, T963A again showed significantly fewer auto- and transphosphorylation activities than the others (15% for KAPP1 and 14% for KAPP2 relative to wild type). Transphosphorylation of the KAPP proteins was reduced in the S936A mutant (36% for KAPP1 and 37% for KAPP2 relative to wild type). The S861A mutant protein is capable of autophosphorylation; however, it was unable to transphosphorylate the KAPP proteins (1.3% for KAPP1 and 1.6% for KAPP2, relative to wild type in the phosphorylation activity). Taken together, the phosphorylation results suggest that Ser-861 and Thr-963 are important for the kinase activity of NARK.

Because both GST-NARK-KD and GST-KAPP1 are substrates for phosphorylation, different time points and different concentrations of GST-NARK-KD were tested in transphosphorylation assays with the GST-KAPP1 protein to determine the level of phosphorylation. Phosphorylation of GST-KAPP1 was increased in a time-dependent manner, and furthermore, this phosphorylation was dependent on the level of GST-NARK-KD autophosphorylation (Fig. 7*A*). Increasing phosphorylation of GST-NARK-KD and GST-KAPP1 was observed when the concentration of GST-NARK-KD was increased, and a stronger phosphorylation of GST-KAPP1 was seen with an equal concentration of both proteins (Fig. 7*B*).

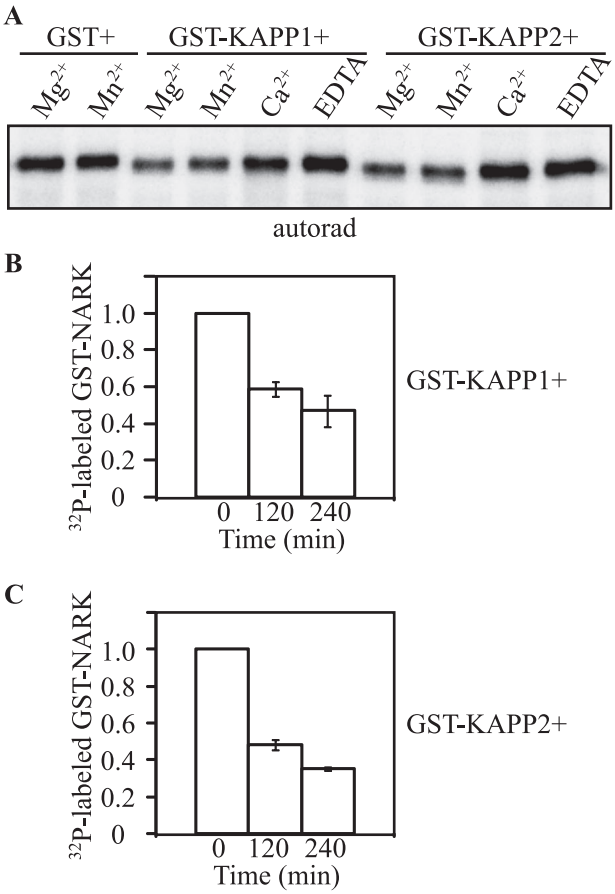

FIGURE 8. **Dephosphorylation of GST-KAPP1 and GST-KAPP2.** *A*, the GST-NARK-KD protein, autophosphorylated on the resin in the presence of [γ-^{32}P]ATP at 25 °C for 90 min, was washed four times to remove the unincorporated isotope, and the protein was eluted. Autophosphorylated GST-NARK-KD was incubated with GST, GST-KAPP1, or GST-KAPP2 in dephosphorylation buffer containing either 10 mM $MgCl_2$, $MnCl_2$, $CaCl_2$, or EDTA at 25 °C for 4 h. *B* and *C*, time course of dephosphorylation of GST-KAPP1 and GST-KAPP2. The ^{32}P-labeled GST-NARK-KD was incubated with either GST-KAPP1 (*B*) or GST-KAPP2 (*C*) in dephosphorylation buffer containing 10 mM $MgCl_2$ from 0 to 240 min. The gels were quantified on the PhosphorImager and analyzed using ImageQuant software.

The Phosphatase Activities of KAPP1 and KAPP2—KAPP is a unique type of 2C protein phosphatase with phosphatase activity demonstrated in *Arabidopsis* (21, 24). To determine whether the *G. max* KAPP1 and KAPP2 proteins are functional protein phosphatases, dephosphorylation assays were carried out. The ^{32}P-labeled GST-NARK-KD protein was incubated with either GST-KAPP1 or GST-KAPP2 in the dephosphorylation buffer containing 10 mM concentrations of different divalent cations. The results showed that the phosphatase activities of both KAPP1 and KAPP2 are dependent on the presence of Mg^{2+} or Mn^{2+} (Fig. 8*A*). Ca^{2+} and EDTA did not affect the phosphatase activities of the KAPP proteins (Fig. 8*A*). The phosphorylated GST-NARK-KD protein was dephosphorylated by both GST-KAPP1 and GST-KAPP2 in a time-dependent manner (Fig. 8, *B* and *C*).

DISCUSSION

Here we characterized the biochemical properties of the *G. max* serine/threonine receptor kinase, NARK, which is responsible for signaling leading to AON in legumes. We confirmed that NARK contains a functional kinase catalytic domain capable of autophosphorylation and autophosphorylation-dependent transphosphorylation *in vitro*. In addition, soybean KAPP proteins were identified to verify transphosphorylation between NARK and the KAPP proteins. Phosphatase activity of the NARK kinase domain by both soybean KAPP proteins was demonstrated *in vitro*, suggesting a complex reciprocal regulatory relay. Because our constructs were not tested by *in planta* assays (requiring stable soybean transformation for transgene expression in leaves, since *NARK* is functionally expressed for AON in the phloem parenchyma of the leaf), these results are only suggestive of a biological function of KAPP in nodulation control.

A kinase-inactivating mutation (K724E) and three missense mutations (E741K, V837A, and R961K) causing the super- or hypernodulation phenotype *in vivo* in three legume species (14, 40, 41), were introduced into the NARK kinase catalytic domain. As expected, these mutations significantly decreased the kinase activity of the protein. Glu-741 in subdomain III and Arg-961 in subdomain XI are nearly invariant among kinases, whereas Val-837 is located between the catalytic loop and the activation loop, where one usually finds a hydrophobic residue, such as Leu, Met, or Ile, but not Ala (46). Arg-961 in subdomain XI forms an ion pair with a nearly invariant glutamic acid in subdomain VIII to stabilize the C-terminal lobe (47). Lys-724 is an invariant residue in subdomain II that contributes to the anchoring and orientation of ATP and interacts with glutamic acid (Glu-741) in subdomain III. We suggest that this loss in the kinase activity results in the failure to send the signal for controlling nodule numbers to the downstream effector proteins, thus resulting in a super- or hypernodulation phenotype (5).

In general, the sequences of the kinase domains of plant RKs are highly conserved. However, the phosphorylation sites and the other regulatory sequences of RKs appear to be variable. In this report, we identified two major phosphorylation sites of the NARK protein, Ser-861 and Thr-963, by mutagenesis and *in vitro* assays.

Ser-861 in the activation loop aligns with Thr-760 in LjSYMRK, Thr-468 in AtSERK1, and Thr-1049 in AtBRI1 (Fig. 9). It has been reported that 82.9% of *Arabidopsis* RKs have serine or threonine at this position according to a PileUP alignment of the entire 610-member RK family (44). Although the GST-NARK-S861A mutant fails to phosphorylate substrates (casein, GST-KAPP1, and GST-KAPP2), mutations on LjSYMRK Thr-760, AtSERK1 Thr-468, and AtBRI1 Thr-1049 significantly decreased both their autophosphorylation and substrate transphosphorylation activities (16, 17, 44). This suggests that at least one of the phosphorylated serine/threonine residues in the activation loop is likely to be required for kinase activation in NARK and several other plant RKs. Phosphorylation in the activation loop shifts the activation loop equilibrium toward the active conformation that accommodates substrate binding (48, 49). In the case of the GST-NARK-S861A mutant, the mutation might permit autophosphorylation (facilitated by the high local concentration of the substrate), but the activity may not be sufficient to phosphorylate other substrates. We were unable to confirm the phosphorylation of NARK at this

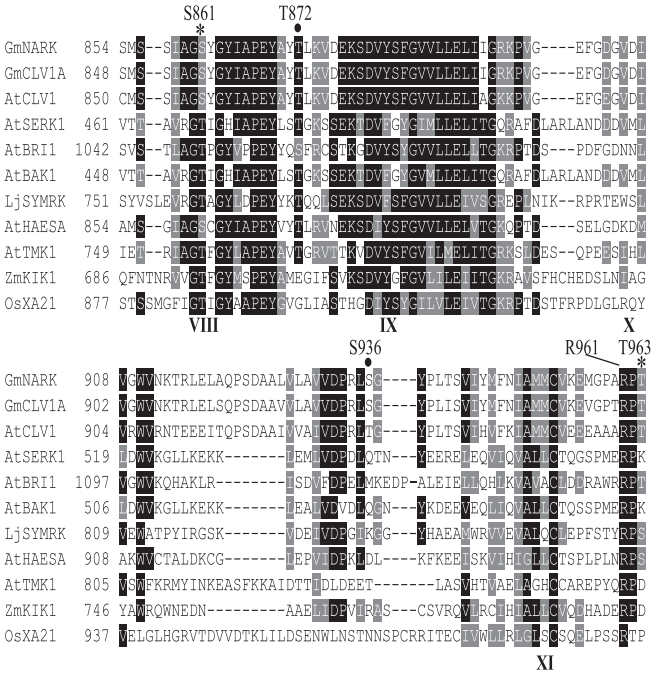

FIGURE 9. **Sequence alignment of a part of the kinase domain from plant receptor kinases.** GmNARK (AY166655), GmCLV1A (AF197946), AtCLV1 (NM_106232), AtSERK1 (NM_105841), AtBRI1 (NM_120100), AtBAK1 (NM_119497), LjSYMRK (AF492655), AtHAESA (NM_118991), AtTMK1 (NM_105286), ZmKIK1 (U82481), and OsXA21 (U37133) were subjected to ClustalW (61), and the multiple alignment output result was decorated by BOXSHADE. Identical and similar amino acids are *shaded black* and *gray*, respectively. Putative phosphorylation sites in NARK are indicated by *asterisks*. An invariant Arg used for MBP-NARK-R961K mutant is indicated. *Roman numerals* show the conserved kinase subdomains.

residue (Ser-861) by mass spectrometry analysis, possibly because the native tryptic peptide is large, which makes it less conducive to ionization by MALDI-TOF/TOF analysis.

Phosphorylation at Thr-963 is supported by mass spectrometry analysis and analysis of the GST-NARK-T963A mutant, which showed a significantly reduced phosphorylation activity *in vitro*. In addition to Ser-861 and Thr-963, our results suggest that the C-terminal and juxtamembrane regions in NARK are targets for phosphorylation. In *Arabidopsis* RKs, the majority of phosphorylation sites *in vivo* are located in the juxtamembrane and the C-terminal regions (50). For example, at least 11 sites of *in vivo* phosphorylation were identified in AtBRI1, and seven of these are located either in the juxtamembrane or the C-terminal domain (44). There are four serine/threonine residues (Ser-972, Ser-977, Thr-979, and Thr-981) and two threonine residues (Thr-676 and Thr-680) and one tyrosine residue (Tyr-664) in the C-terminal and the juxtamembrane domains of NARK, respectively. The truncated MBP-NARK-KD proteins lacking either the C-terminal or the juxtamembrane domain (MBP-NARK(-CT) and MBP-NARK(-JM), respectively) showed fewer autophosphorylation activities compared with the wild-type MBP-NARK-KD *in vitro* (supplemental Fig. 1*B*). Consistent with this result, mass spectrometry analysis showed that the adjacent tryptic peptide (aa 966–987) contained one or two phosphate modifications in the C-terminal region. Also, Tyr-664 might be a possible phosphorylation site in the juxtamembrane region of NARK, based on the result of mass spectrometry, although we could not exclude the possibility that a serine in the GST linker is phosphorylated. Furthermore, either Ser-731 or Tyr-736 is also a probable NARK phosphorylation site. However, the GST-NARK-S731A mutation had little effect on auto- or transphosphorylation ability.

A limited number of RKs have been isolated and characterized from plants in the last 15 years. In some signaling pathways, autophosphorylation plays a central role in their regulation. Our results show that the GST-NARK-KD protein appears to be able to phosphorylate the kinase-inactive MBP-NARK-K724E mutant. This suggests that *in vitro* autophosphorylation of NARK most likely takes place in *trans*, similar to other plant RKs, such as HAESA, CLV1, SERK1, and SYMRK (16, 17, 19, 32).

In plants, the brassinosteroid pathway is one of the best understood signal transduction pathways. Recent studies demonstrated that BRI1 interacts with BRI1-associated receptor kinase 1 (BAK1), and BRI1/BAK1 dimerization and kinase activation are induced by brassinosteroid, although it is not fully understood whether dimerization of BRI1/BAK1 is the cause or result of ligand-induced activation of BRI1 kinase (51). In addition, it has been proposed that CLV1 forms a heterodimer with the CLV2 receptor-like protein (52, 53). Thus, we can speculate that NARK may also dimerize or oligomerize with other RK(s). In *L. japonicus*, the hypernodulation phenotype *klavier* mutant shows other phenotypes, such as a lesser number of lateral roots, fasciated stems, increased number of flowers, reduced xylogenesis, and bifurcated pistils that have not been observed in *har1* (54). Although the *klavier* phenotype is not identical to the *har1/nark* phenotype, some aspects, such as the shoot control phenotype, root growth alterations, and reduced nitrate sensitivity for nodulation are common between the two hypernodulation mutants. Therefore, KLAVIER is most likely involved directly or indirectly in the same signaling pathway.

Knowing how NARK signaling is activated and regulated is important for understanding how the communication between the root and the shoot is directed in AON. Therefore, in addition to the autophosphorylation activity of NARK, we were interested in the downstream components of the NARK signaling pathway. We isolated the soybean homologues of KAPP as possible interacting partners of NARK. As expected from its allotetraploid genome, we found that soybean possesses two copies of *KAPP*, namely *KAPP1* and *KAPP2*. We also isolated the *L. japonicus* homologue of *KAPP* (GenBank™ accession number EU350556), and Southern blot analysis confirmed that *L. japonicus*, like *Arabidopsis* and maize, had a single copy (Fig. 5*C*). Duplication of *KAPP* genes can be explained by considering the evolution of soybean (*G. max*), which is highly complicated by at least two rounds of polyploidization (55). It has been proposed that all extant species of *Glycine* are the products of an ancient genome duplication event (56). Results of RFLP mapping indicate that most probes are duplicated an average of 2.55 times in the soybean genome (57). Therefore, most of the genes in soybean have at least two copies. For example, *NARK* (previously known as soybean *CLV1B*) and soybean *CLV1A* share 92% sequence in the coding regions (58). However, despite the high sequence identity, CLV1A does not complement NARK, since *nark* mutants segregate as classical Mendelian recessives.

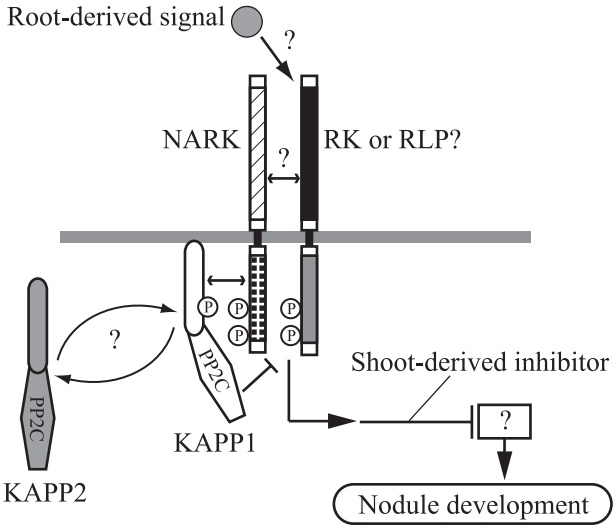

FIGURE 10. **Predicted model of the NARK signal transduction pathway.** After the infection of soybean with *Rhizobium*, a root-derived signal is transported to the shoot. Ligand binding facilitates the dimerization of NARK with a receptor kinase or a receptor-like protein (*RLP*), in the phloem parenchyma of vascular bundles in the leaf (60), allowing reciprocal phosphorylation in the NARK/RK or the NARK/RLP dimer for activation. The KI domain of KAPP1 and KAPP2 is transphosphorylated by the NARK kinase domain. The PP2C domain of the KAPP1 and KAPP2 in turn dephosphorylates NARK receptor. The resulting signal is relayed from NARK to several unknown downstream effectors, which results in the production of a shoot-derived inhibitor to control nodule development.

In this report, we failed to find significant functional differences between KAPP1 and KAPP2 for *in vitro* phosphorylation by NARK, suggesting functional redundancy. Both functional KAPP proteins were phosphorylated by the NARK kinase catalytic domain, and KAPP1 dephosphorylated the autophosphorylated NARK similarly to KAPP2 in the presence of Mg^{2+} and Mn^{2+} *in vitro*. In addition to the evidence presented here, we found that a signal anchor and five essential residues in the KI-FHA domain, corresponding to Gly-211, Arg-212, Ser-226, His-229, and Asn-250 in *Arabidopsis* KAPP (27, 28), are completely conserved between KAPP1 and KAPP2. Furthermore, 11 conserved PP2C motifs of KAPP1 and KAPP2 are highly conserved. Thus, we hypothesize that KAPP1 will complement KAPP2 and *vice versa* and that both of them play roles as negative regulators of NARK (Fig. 10). Expression of *KAPP1* and *KAPP2* was confirmed in shoot tips, leaves, roots, and nodules of the soybean plant inoculated with rhizobia by quantitative RT-PCR (data not shown). Because of the ubiquitous expression of *KAPP1* and *KAPP2*, they are also likely to function in several signaling pathways in soybean as well as *KAPPs* in other plants, such as *Arabidopsis* and maize (22).

Most of the upstream and downstream components in the NARK pathway remain to be identified. Finding a root-derived signal and a ligand of the NARK receptor complex is critical to understanding the signaling mechanism of the NARK receptor. We postulate that our results shown here reflect properties of other AON receptor kinases, proving a general legume paradigm for kinase function in systemic control of nodule proliferation (and possibly root development). Further biochemical experiments, structural studies, interaction studies, such as yeast two-hybrid assays, and *in vivo* cell biology experiments will give us strong clues for understanding the role of the NARK receptor in the signaling pathway controlling systemic nodulation and root growth control (59, 60).

Acknowledgments—We are grateful to Dr. Ross Brinkworth for help with phosphorylation site analysis. We thank Dr. Thierry Lonhienne, Dr. Paul Scott, and Dr. Gustavo Gualtieri for helpful discussions, editing, and supervision of phosphorylation assays. Dr. Peter Milburn at the Biomolecular Resource Facility at the Australian National University provided MALDI-TOF/TOF analysis and aided in the identification of phosphopeptides.

REFERENCES

1. Shiu, S. H., and Bleecker, A. B. (2001) *Proc. Natl. Acad. Sci. U. S. A.* **98,** 10763–10768
2. Clark, S. E., Williams, R. W., and Meyerowitz, E. M. (1997) *Cell* **89,** 575–585
3. Fletcher, L. C., Brand, U., Running, M. P., Simon, R., and Meyerowitz, E. M. (1999) *Science* **283,** 1911–1914
4. Jeong, S., Trotochaud, A. E., and Clark, S. E. (1999) *Plant Cell* **11,** 1925–1933
5. Kinkema, M., Scott, P. T., and Gresshoff, P. M. (2006) *Funct. Plant Biol.* **33,** 707–721
6. Madsen, E. B., Madsen, L. H., Radutoiu, S., Olbryt, M., Rakwalska, M., Szczyglowski, K., Sato, S., Kaneko, T., Tabata, S., Sandal, N., and Stougaard, J. (2003) *Nature* **425,** 637–640
7. Radutoiu, S., Madsen, L. H., Madsen, E. B., Felle, H. H., Umehara, Y., Gronlund, M., Sato, S., Nakamura, Y., Tabata, S., Sandal, N., and Stougaard, J. (2003) *Nature* **425,** 585–592
8. Searle, I. R., Men, A. E., Laniya, T. S., Buzas, D. M., Iturbe-Ormaetxe, I., Carroll, B. J., and Gresshoff, P. M. (2003) *Science* **299,** 109–112
9. Stracke, S., Kistner, C., Yoshida, S., Mulder, L., Sato, S., Kaneko, T., Tabata, S., Sandal, N., Stougaard, J., Szczyglowski, K., and Parniske, M. (2002) *Nature* **417,** 959–962
10. Imaizumi-Anraku, H., Takeda, N., Charpentier, M., Perry, J., Miwa, H., Umehara, Y., Kouchi, H., Murakami, Y., Mulder, L., Vickers, K., Pike, J., Downie, J. A., Wang, T., Sato, S., Asamizu, E., Tabata, S., Yoshikawa, M., Murooka, Y., Wu, G. J., Kawaguchi, M., Kawasaki, S., Parniske, M., and Hayashi, M. (2005) *Nature* **433,** 527–531
11. Levy, J., Bres, C., Geurts, R., Chalhoub, B., Kulikova, O., Duc, G., Journet, E. P., Ane, J. M., Lauber, E., Bisseling, T., Denarie, J., Rosenberg, C., and Debelle, F. (2004) *Science* **303,** 1361–1364
12. Krusell, L., Madsen, L. H., Sato, S., Aubert, G., Genua, A., Szczyglowski, K., Duc, G., Kaneko, T., Tabata, S., de Bruijn, F., Pajuelo, E., Sandal, N., and Stougaard, J. (2002) *Nature* **420,** 422–426
13. Nishimura, R., Hayashi, M., Wu, G. J., Kouchi, H., Imaizumi-Anraku, H., Murakami, Y., Kawasaki, S., Akao, S., Ohmori, M., Nagasawa, M., Harada, K., and Kawaguchi, M. (2002) *Nature* **420,** 426–429
14. Schnabel, E., Journet, E. P., de Carvalho-Niebel, F., Duc, G., and Frugoli, J. (2005) *Plant Mol. Biol.* **58,** 809–822
15. Wang, X. L., Li, X. Q., Meisenhelder, J., Hunter, T., Yoshida, S., Asami, T., and Chory, J. (2005) *Dev. Cell* **8,** 855–865
16. Shah, K., Vervoort, J., and de Vries, S. C. (2001) *J. Biol. Chem.* **276,** 41263–41269
17. Yoshida, S., and Parniske, M. (2005) *J. Biol. Chem.* **280,** 9203–9209
18. Liu, G. Z., Pit, L. Y., Walker, J. C., Ronald, P. C., and Song, W. Y. (2002) *J. Biol. Chem.* **277,** 20264–20269
19. Williams, R. W., Wilson, J. M., and Meyerowitz, E. M. (1997) *Proc. Natl. Acad. Sci. U. S. A.* **94,** 10467–10472
20. Stone, J. M., Trotochaud, A. E., Walker, J. C., and Clark, S. E. (1998) *Plant Physiol.* **117,** 1217–1225
21. Stone, J. M., Collinge, M. A., Smith, R. D., Horn, M. A., and Walker, J. C. (1994) *Science* **266,** 793–795
22. Braun, D. M., Stone, J. M., and Walker, J. C. (1997) *Plant J.* **12,** 83–95
23. Gomez-Gomez, L., Bauer, Z., and Boller, T. (2001) *Plant Cell* **13,** 1155–1163

24. Shah, K., Russinova, E., Gadella, T. W., Jr., Willemse, J., and De Vries, S. C. (2002) *Genes Dev.* **16,** 1707–1720
25. Ding, Z., Wang, H., Liang, X., Morris, E. R., Gallazzi, F., Pandit, S., Skolnick, J., Walker, J. C., and Doren, S. R. (2007) *Biochemistry* **46,** 2684–2696
26. van der Knaap, E., Song, W. Y., Ruan, D. L., Sauter, M., Ronald, P. C., and Kende, H. (1999) *Plant Physiol.* **120,** 559–569
27. Li, J., Smith, G. P., and Walker, J. C. (1999) *Proc. Natl. Acad. Sci. U. S. A.* **96,** 7821–7826
28. Li, J., Lee, G. I., Van Doren, S. R., and Walker, J. C. (2000) *J. Cell Sci.* **113,** 4143–4149
29. Guan, K. L., and Dixon, J. E. (1991) *Anal. Biochem.* **192,** 262–267
30. Adereth, Y., Champion, K. J., Hsu, T., and Dammai, V. (2005) *BioTechniques* **38,** 864–868
31. Altschul, S. F., Gish, W., Miller, W., Myers, E. W., and Lipman, D. J. (1990) *J. Mol. Biol.* **215,** 403–410
32. Horn, M. A., and Walker, J. C. (1994) *Biochim. Biophys. Acta* **1208,** 65–74
33. Skolnick, J., Kihara, D., and Zhang, Y. (2004) *Proteins* **56,** 502–518
34. Zhang, Y., and Skolnick, J. (2004) *Proc. Natl. Acad. Sci. U. S. A.* **101,** 7594–7599
35. Huse, M., Chen, Y. G., Massague, J., and Kuriyan, J. (1999) *Cell* **96,** 425–436
36. Guex, N., and Peitsch, M. C. (1997) *Electrophoresis* **18,** 2714–2723
37. Djordjevic, M. A., Oakes, M., Li, D. X., Hwang, C. H., Hocart, C. H., and Gresshoff, P. M. (2007) *J. Proteome Res.* **6,** 3771–3779
38. Natera, S. H. A., Guerreiro, N., and Djordjevic, M. A. (2000) *Mol. Plant-Microbe Interact.* **13,** 995–1009
39. Djordjevic, M. A., Chen, H. C., Natera, S., Van Noorden, G., Menzel, C., Taylor, S., Renard, C., Geiger, O., and Weiller, G. F. (2003) *Mol. Plant-Microbe Interact.* **16,** 508–524
40. Carroll, B. J., McNeil, D. L., and Gresshoff, P. M. (1985) *Proc. Natl. Acad. Sci. U. S. A.* **82,** 4162–4166
41. Penmetsa, R. V., Frugoli, J. A., Smith, L. S., Long, S. R., and Cook, D. R. (2003) *Plant Physiol.* **131,** 998–1008
42. Brinkworth, R. I., Breinl, R. A., and Kobe, B. (2003) *Proc. Natl. Acad. Sci. U. S. A.* **100,** 74–79
43. Blom, N., Gammeltoft, S., and Brunak, S. (1999) *J. Mol. Biol.* **294,** 1351–1362
44. Wang, X. F., Goshe, M. B., Soderblom, E. J., Phinney, B. S., Kuchar, J. A., Li, J., Asami, T., Yoshida, S., Huber, S. C., and Clouse, S. D. (2005) *Plant Cell* **17,** 1685–1703
45. van der Knaap, E., Song, W. Y., Ruan, D. L., Sauter, M., Ronald, P. C., and Kende, H. (1999) *Plant Physiol.* **120,** 559–570
46. Hanks, S. K., Quinn, A. M., and Hunter, T. (1988) *Science* **241,** 42–52
47. Schenk, P. W., and Snaar-Jagalska, B. E. (1999) *Biochim. Biophys. Acta* **1449,** 1–24
48. Johnson, L. N., Noble, M. E. M., and Owen, D. J. (1996) *Cell* **85,** 149–158
49. Kobe, B., and Kemp, B. E. (2004) in *Handbook of Cell Signaling*, Vol. 1, 1st Ed., pp. 539–542, Academic Press, Inc., San Diego, CA
50. Nuhse, T. S., Stensballe, A., Jensen, O. N., and Peck, S. C. (2004) *Plant Cell* **16,** 2394–2405
51. Wang, Z. Y., Wang, Q. M., Chong, K., Wang, F. R., Wang, L., Bai, M. Y., and Jia, C. G. (2006) *Cell Res.* **16,** 427–434
52. Fletcher, J. C. (2002) *Annu. Rev. Plant Biol.* **53,** 45–66
53. Sharma, V. K., Carles, C., and Fletcher, J. C. (2003) *Proc. Natl. Acad. Sci. U. S. A.* **100,** 11823–11829
54. Oka-Kira, E., Tateno, K., Miura, K., Haga, T., Hayashi, M., Harada, K., Sato, S., Tabata, S., Shikazono, N., Tanaka, A., Watanabe, Y., Fukuhara, I., Nagata, T., and Kawaguchi, M. (2005) *Plant J.* **44,** 505–515
55. Walling, J. G., Shoemaker, R., Young, N., Mudge, J., and Jackson, S. (2006) *Genetics* **172,** 1893–1900
56. Shoemaker, R. C., Schlueter, J., and Doyle, J. J. (2006) *Curr. Opin. Plant Biol.* **9,** 104–109
57. Shoemaker, R. C., Polzin, K., Labate, J., Specht, J., Brummer, E. C., Olson, T., Young, N., Concibido, V., Wilcox, J., Tamulonis, J. P., Kochert, G., and Boerma, H. R. (1996) *Genetics* **144,** 329–338
58. Yamamoto, E., Karakaya, H. C., and Knap, H. T. (2000) *Biochim. Biophys. Acta* **1491,** 333–340
59. Buzas, D. M., and Gresshoff, P. M. (2007) *J. Plant Physiol.* **164,** 452–459
60. Nontachalyapoom, S., Scott, P. T., Men, A. E., Kinkema, M., Schenk, P. M., and Gresshoff, P. M. (2007) *Mol. Plant-Microbe Interact.* **20,** 769–780
61. Thompson, J. D., Higgins, D. G., and Gibson, T. J. (1994) *Nucleic Acids Res.* **22,** 4673–4680

Supplemental Data 1. *A*, Schematic diagram of the wild-type MBP-NARK-KD and its truncated constructs used in the experiment (B). *B*, Autophosphorylation activities of MBP-NARK-KD protein, MBP-NARK C-terminal region deletion mutant (MBP-NARK(-CT)), and MBP-NARK juxtamembrane region deletion mutant (MBP-NARK(-JM)). After 60-min incubation at 25°C, protein samples were separated by SDS-PAGE and the radioactive bands were detected by the PhosphorImager. Coomassie staining of the same gel is shown (CBB).

Supplemental Data 1

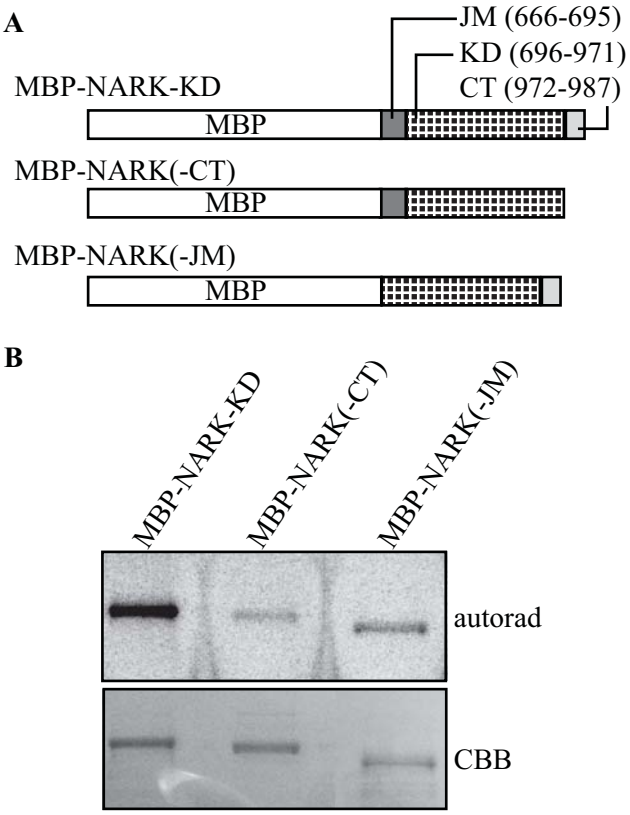

Soybean Nodule Autoregulation Receptor Kinase Phosphorylates Two Kinase-associated Protein Phosphatases *in Vitro*

Akira Miyahara, Tripty A. Hirani, Marie Oakes, Attila Kereszt, Bostjan Kobe, Michael A. Djordjevic and Peter M. Gresshoff

J. Biol. Chem. 2008, 283:25381-25391.
doi: 10.1074/jbc.M800400200 originally published online July 7, 2008
